



Received: December 21, 2024
Revised: April 14, 2025
Accepted: May 1, 2025

Corresponding author:

Anže Jerman, M.D.
Department of Maxillofacial and Oral Surgery,
University Medical Center Ljubljana, Hrvatski
trg 6, 1000 Ljubljana, Slovenia
Tel: +386-01 543 73 02
Fax: +386-01 543 73 01
Email: anze.jerman@mf.uni-lj.si
ORCID: <https://orcid.org/0000-0003-0816-3800>



© The Korean Society of Anesthesiologists, 2025

© This is an open-access article distributed under the terms of the Creative Commons Attribution Non-Commercial License (<http://creativecommons.org/licenses/by-nc/4.0/>) which permits unrestricted non-commercial use, distribution, and reproduction in any medium, provided the original work is properly cited.

Injectate distribution patterns in posterior infrazygomatic and transoral approaches to the pterygopalatine fossa

Anže Jerman^{1,2}, Luka Pušnik², Erika Cvetko², Nejc Umek², Žiga Snoj^{3,4}

¹Department of Maxillofacial and Oral Surgery, University Medical Center Ljubljana, ²Institute of Anatomy, University of Ljubljana Faculty of Medicine, ³Institute of Radiology, University Medical Center Ljubljana, ⁴Department of Radiology, University of Ljubljana Faculty of Medicine, Ljubljana, Slovenia

Background: Injectate distribution patterns in the pterygopalatine fossa may differ based on the drug administration approach used. This study primarily aimed to assess and compare injectate distribution following the posterior infrazygomatic and transoral approaches. The secondary aim was to evaluate the safety of both approaches.

Methods: Injectate distribution patterns were evaluated in 13 cadaveric head specimens. The vessels were perfused with a gelatin-based solution containing an iodinated contrast agent. The ultrasound-guided posterior infrazygomatic approach and transoral approach were performed on contralateral sides, and needle placement was confirmed using computed tomography (CT). A methylene blue and iodinated contrast agent solution was administered following successful needle placement. Injectate distribution and injuries were assessed via CT and anatomical dissection.

Results: With the posterior infrazygomatic approach, methylene blue consistently stained the maxillary artery and nerve, sphenopalatine ganglion, and lateral pterygoid muscle, whereas with the transoral approach, it most frequently surrounded the maxillary artery and structures within the greater palatine canal. The iodinated contrast agent was distributed predominantly along the needle trajectories for both approaches. Injuries to the maxillary artery and facial nerve were documented following the posterior infrazygomatic approach, whereas injury to the lateral pterygoid plate was observed following the transoral approach.

Conclusions: With the posterior infrazygomatic approach, contrast agent encompassed the entire pterygopalatine fossa, whereas the transoral approach yielded a more localized distribution, primarily within the inferior portion and greater palatine canal. These differences in distribution patterns should guide the selection of the most appropriate approach based on the specific clinical indication.

Keywords: Ganglion; Ganglion cysts; Local anesthetics; Maxillary artery; Maxillary nerve; Pterygopalatine fossa; Sphenopalatine ganglion block.

Introduction

The pterygopalatine fossa is an inverted pyramid-shaped space that serves as a crucial distribution center for the innervation and vascular supply of deep facial structures [1]. Housing the sphenopalatine ganglion, the maxillary nerve and its branches, parasympathetic nerve fibers, and a segment of the maxillary artery, the pterygopalatine fossa plays

a significant role in the pathogenesis of head and facial pain [2,3]. In recent decades, performing a blockade of neurological structures within the pterygopalatine fossa has emerged as a valuable technique, especially for the treatment of facial pain associated with trigeminal neuralgia, acute migraine headaches [4], post-dural puncture headaches [5], pain management after adenotonsillectomy [6], and perioperative analgesia during cleft palate repair [7]. The application of anesthetics into the fossa has been shown to successfully reduce complications and the need for systemic steroids [4,7]. In addition, the administration of vasoconstrictors combined with local anesthetics into the pterygopalatine fossa during paranasal sinus surgery can significantly reduce intraoperative bleeding [8]. Consequently, various approaches for drug administration into the pterygopalatine fossa have been proposed and explored in recent years.

However, no consensus currently exists on the optimal approach to access the pterygopalatine fossa, which likely reflects institutional preferences and diverse clinical indications [9].

Three main approaches via the pterygomaxillary fissure have been described [4,10,11]. One such approach is the posterior infrazygomatic approach, which offers the greatest needle mobility and widest range of access, but carries a higher risk of injury to the maxillary artery, as demonstrated by virtual reality studies [12,13]. With this approach, the needle does not directly enter the pterygopalatine fossa but instead traverses the lateral pterygoid muscle, passes over the lateral pterygoid plate, and is ultimately positioned adjacent to the pterygopalatine fossa [9]. This indirect pathway has raised doubts about the adequate spread of the injectate into the pterygopalatine fossa [9,10].

Conversely, with the transoral approach, anesthetics are delivered through the oral cavity via the greater palatine canal, with the needle tip positioned in the inferior portion of the pterygopalatine fossa [14]. This technique may result in a distinct distribution pattern compared with approaches through the pterygomaxillary fissure, potentially targeting neurovascular structures located in the inferior portion of the pterygopalatine fossa more effectively, such as the greater and lesser palatine nerves, and the maxillary artery [14–16]. The resulting differences in anesthetic or vasoconstrictor distribution may be used to guide the selection of the most appropriate approach for specific clinical conditions.

To date, no studies have evaluated the injectate distribution patterns associated with the posterior infrazygomatic and transoral approaches [9]. Therefore, the primary aim of this study was to compare the injectate distribution within the pterygopalatine fossa following the posterior infrazygomatic and transoral approaches. The secondary aim was to assess the safety of both approaches.

Materials and Methods

Ethics committee approval

This study was conducted on 13 fresh (less than 24 hours post-mortem) cadaveric heads (six female and seven male, aged 82.4 ± 6.7 years) obtained through a willed body donation program at the Institute of Anatomy, Faculty of Medicine, University of Ljubljana. The donors provided informed consent for the donation of their bodies for research purposes. Specimens with documented traumatic injuries to the head or neck region, or a history of surgical procedures in this area, were excluded. This study was approved by the National Medical Ethics Committee of the Republic of Slovenia (Permit no: 0120-538/2019/4).

Specimen preparation

Specimen preparation involved perfusion of the arteries and veins with an iodinated contrast agent and dyes. A 100 ml solution was prepared that contained 10 g of gelatin (Gelatin Powder, Sigma Aldrich GmbH), 15 ml of iohexol (Visipaque 320, GE Healthcare), saline solution, and acrylic paints (red for arteries and blue for veins) [17,18]. Approximately 50–60 ml of the prepared solution was injected into the common carotid arteries and internal jugular veins using a syringe. The vessels were immediately ligated, and the specimens were placed in the supine position for 3 hours to allow the gelatin to solidify.

Posterior infrazygomatic and transoral approach attempts

Both approaches for accessing the pterygopalatine fossa were attempted on each specimen. First, an experienced interventional and musculoskeletal radiologist performed the ultrasound-guided posterior infrazygomatic approach. An ultrasound machine (Arietta 850, Fujifilm VisualSonics) equipped with an SML44 linear probe (22-2 MHz) was used. The specimen was positioned in the lateral position and the probe was placed longitudinally below the zygomatic arch, enabling visualization of the maxillary tuberosity, lateral pterygoid muscle, and lateral plate of the pterygoid process. A 25-gauge needle was inserted inferior to the zygomatic arch, just anterior to the mandibular condyle. Following needle placement deep to the lateral pterygoid muscle, computed tomography (CT) imaging was performed. If the needle tip was confirmed to be positioned at the pterygomaxillary fissure or within the pterygopalatine fossa (as both represent a feasible needle end position in the clinical setting) the study proceeded using the transoral ap-

proach; otherwise, the needle was repositioned. The sides used for the posterior infrazygomatic and transoral approaches were randomly assigned to account for potential anatomical variations.

An experienced otorhinolaryngology (ENT) surgeon performed the transoral approach through the greater palatine canal on the contralateral side. The head was placed in the supine position. The oral cavity was opened using a retractor followed by manual palpation to locate the greater palatine canal [14]. A 22-gauge needle turned at a 45° angle at a distance of 25 mm from its tip [19] was then inserted into the greater palatine canal. Consistently angling the needle at 45° ensured that it was always positioned at the same depth (25 mm). After needle placement, a repeat CT was performed to confirm the position of the needle tip within the pterygopalatine fossa. If the needle tip was within the pterygopalatine fossa, the standard solution was injected on both sides to ensure timing consistency; otherwise, the approach was repeated until needle placement within the pterygopalatine fossa was achieved.

The standard solution was prepared using 1% methylene blue and iohexol (Visipaque 320, GE HealthCare) at a 1:1 ratio. Based on the reported volume of the pterygopalatine fossa [20], 1 ml of the standard solution was injected for each approach and the needle was immediately sealed with a stopper.

Evaluation of injectate distribution via computed tomography

CT imaging was performed to verify the needle position and again after injectate administration. A SOMATOM Definition Flash CT scanner (Siemens) was used with the following parameters: tube voltage, 120 kV; effective current, 70–150 mAs pixel size, 0.383 mm × 0.383 mm; pitch, 0.65; slice thickness, 0.75 mm, and interslice distance, 0.9 mm.

To evaluate the injectate distribution, the needle trajectory was initially traced to the transverse and sagittal sections and the presence of contrast within the infratemporal fossa or greater palatine canal was assessed. To determine distribution in the infratemporal fossa, the proximity of the injectate to the medial and lateral pterygoid muscles was evaluated, whereas contrast extending inferiorly as a continuation of the pterygopalatine fossa was classified as being within the greater palatine canal. The presence of contrast within the pterygopalatine fossa was determined based on its distribution near key anatomical landmarks. If contrast was observed in direct contact with the foramen rotundum, it was considered to surround the maxillary nerve. Contrast in direct contact with the pterygoid canal was considered indicative of proximity to the vidian nerve and sphenopalatine ganglion, whereas the presence of

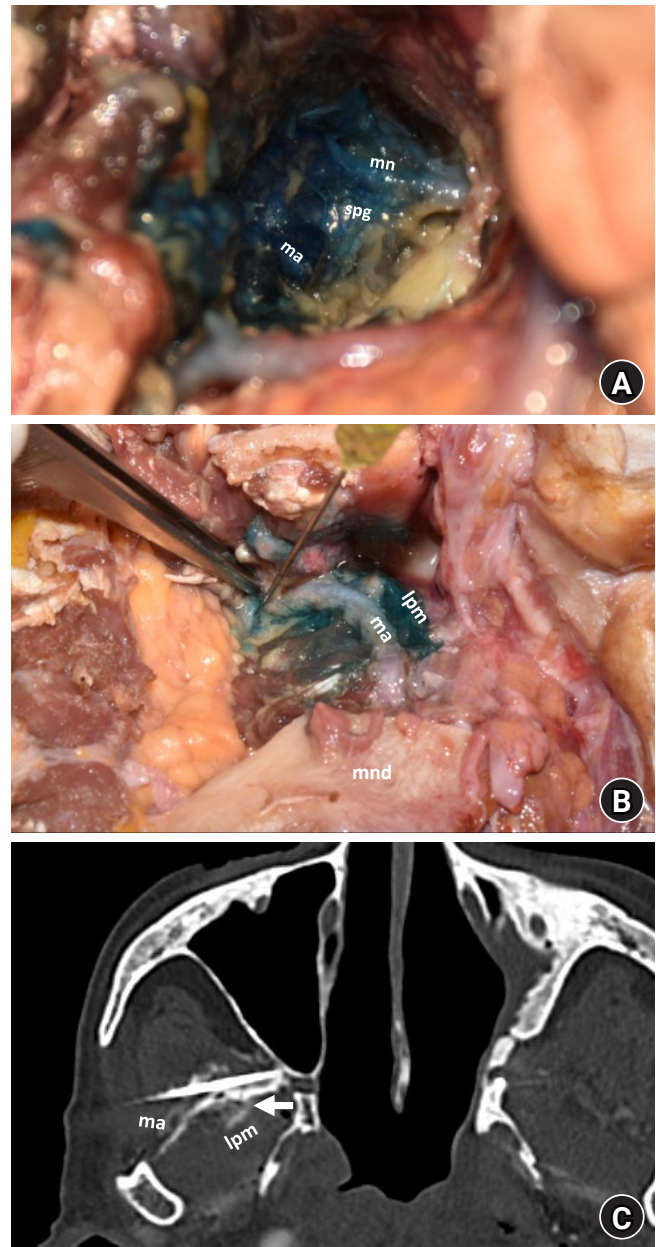


Fig. 1. Distribution pattern following the posterior infrazygomatic approach. (A) Methylene blue staining of the majority of the contents of the pterygopalatine fossa, including the maxillary nerve, maxillary artery, and sphenopalatine ganglion. (B) Methylene blue distribution within the infratemporal fossa, surrounding the lateral pterygoid muscle and maxillary artery. (C) Iodinated contrast agent spread along the needle trajectory (arrows) encompassing the maxillary artery within the infratemporal fossa and lateral pterygoid muscle. mn: maxillary nerve, spg: sphenopalatine ganglion, ma: maxillary artery, lpm: lateral pterygoid muscle, mnd: mandible.

contrast in direct contact with the previously opacified maxillary artery indicated its distribution near the artery. Finally, the orbit and middle cranial fossa were evaluated for the presence of contrast, particularly at the bony landmarks of the inferior orbital fis-

sure and Meckel's cave, respectively.

The CT images were also inspected for any signs of injury to the bones or potential penetration of blood vessels (as evidenced by iodinated contrast within the vessels). The distance from the skin to the needle tip was measured for the posterior infrazygomatic approach, and the shortest distance from the needle tip to the maxillary artery was measured for the transoral approach.

Evaluation of injectate distribution via specimen dissection

Immediately after CT imaging, the heads were placed in the supine position, and layer-by-layer dissection was initiated by an experienced ENT surgeon. The delay between the CT scan and the initiation of anatomical dissection was up to one hour.

A lazy-S incision was made, and a cutaneous flap was elevated over the parotid gland. Superficial structures including the parotid duct, branches of the facial nerve, parotid gland, and superficial arteries (temporal and transverse facial arteries) were inspected for possible damage. The facial nerve was identified, its branches were traced to the site of the needle, and any observed injuries were documented. The parotid gland was removed and skeletonization of the mandibular ramus was performed on the external aspect. The mandible was then transected near the mandibular angle, followed by the disarticulation of the temporomandibular joint. The medial pterygoid muscle was detached, allowing for the complete removal of the mandibular ramus. Dissection continued with a detailed assessment of the infratemporal fossa while tracing the needle. The distribution pattern of the injectate within the infratemporal fossa was assessed by evaluating the medial and lateral pterygoid muscles. The maxillary artery was followed into the pterygopalatine fossa and the surrounding tissues were gradually removed. The maxillary artery was assessed for possible injury. The needle was removed before evaluating the pterygopalatine fossa distribution pattern. Distribution within the pterygopalatine fossa was then evaluated by assessing the sphenopalatine ganglion and maxillary artery and nerve. Using a chisel, the foramen rotundum and greater palatine canal were opened and the injectate distribution patterns within the middle cranial fossa and greater palatine canal were evaluated, respectively. The inferior orbital fissure was inspected for orbital spread.

Identical procedural steps were followed on the contralateral side, where the transoral approach had been performed.

Statistical analysis

Data are presented as absolute numbers with proportions or

standard deviations (\pm SD), where appropriate. The neurovascular injury and injectate distribution analyses were conducted and presented separately for specimen dissections and CT imaging. The groups (posterior infrazygomatic vs. transoral approach) were compared using Fisher's exact test. Statistical analyses were performed using GraphPad Prism 10 (GraphPad Software Inc.), and the significance level was set at $P < 0.05$.

Results

Posterior infrazygomatic approach

For the majority of the attempts (11/13), the needle was positioned at the level pterygomaxillary fissure. The mean distance from the skin to the needle tip measured on CT was 53 ± 9 mm. Methylene blue consistently stained the maxillary artery and nerve, vidian nerve, and the sphenopalatine ganglion (Fig. 1A). Distribution was observed near the lateral pterygoid muscle in all specimens (Fig. 1B), whereas the medial pterygoid muscle was stained in approximately half of the specimens (Table 1). The distribution of the iodinated contrast agent exhibited a similar pattern and was predominantly observed along the needle trajectory (Fig. 1C).

For the remaining two attempts, the needle was positioned within the pterygopalatine fossa (4–5 mm) and methylene blue exhibited a distribution pattern similar to that with the pterygomaxillary fissure needle placement. However, the iodinated contrast agent showed a different pattern, consistently surrounding the sphenopalatine ganglion, maxillary nerve, and pterygoid canal (Table 1).

No orbital spread was observed in any of the anatomical dissections or CT imaging. Methylene blue spread was detected through the foramen rotundum in one specimen, although the Gasserian ganglion remained unstained.

During anatomical dissection, one injury to the temporal branch of the facial nerve was identified (Fig. 2A) and a puncture injury to the pterygoid portion of the maxillary artery was observed in another specimen (Fig. 2B), later confirmed on CT. No additional injuries were identified.

Transoral approach

Methylene blue distribution was most frequently observed within the the greater canal and near the maxillary artery (Fig. 3). Methylene blue was also observed near the sphenopalatine ganglion and maxillary nerve in approximately half of the attempts, whereas iodinated contrast was detected predominantly along the

Table 1. Comparison of Injectate Distribution Patterns between the Posterior Infrazygomatic and Transoral Approaches to the Pterygopalatine Fossa

Anatomical location	Posterior infrazygomatic approach		Transoral approach	
	Dissection	CT	Dissection	CT
Orbit	0 (0)	0 (0)	0 (0)	0 (0)
Middle cranial fossa	1 (8)	0 (0)	0 (0)	0 (0)
Lateral pterygoid muscle	13 (100)*	13 (100) [†]	7 (54)	7 (54)
Medial pterygoid muscle	8 (62)*	0 (0)	1 (8)	1 (8)
Sphenopalatine ganglion	13 (100)*	2 (15)	7 (54)	2 (15)
Maxillary nerve	12 (92)*	2 (15)	6 (46)	0 (0)
Greater palatine canal	0 (0)*	0 (0) [†]	13 (100)	13 (100)
Pterygoid canal	12 (92)	2 (15)	7 (54)	2 (15)
Adjacent to maxillary artery in PPF	13 (100)	4 (31) [†]	11 (85)	10 (77)

Values are presented as number (%). Statistical analyses were performed using the Fisher's exact test separately for anatomical dissection and CT evaluations. CT: computed tomography. *Significant difference between the approaches (anatomical dissection). [†]Significant difference between the approaches (CT evaluation).

needle trajectory and near the lateral pterygoid muscle (Table 1).

In one attempt, the needle had penetrated the lateral pterygoid plate (Fig. 2C), allowing the injectate to spread into the medial pterygoid muscle. With the exception of this specimen, the needle tip was consistently positioned within the inferior portion of the pterygopalatine fossa. On CT, the measured distance from the needle tip to the maxillary artery was 2 ± 1 mm.

No other injuries to the superficial or neurovascular structures were observed in any of the anatomical dissections or CT imaging.

Discussion

This study evaluated injectate distribution patterns following two distinct approaches targeting the pterygopalatine fossa. With the posterior infrazygomatic approach, the injectate spread encompassed the entire pterygopalatine fossa, whereas the transoral approach resulted in the injectate being predominantly distributed in the inferior portion of the pterygopalatine fossa and within the greater palatine canal. In two specimens subjected to the posterior infrazygomatic approach, the needle perforated either the maxillary artery or facial nerve, and injury to the lateral pterygoid plate was observed in one specimen following the transoral approach.

In the posterior infrazygomatic approach, the contrast distribution was most prominent near the lateral pterygoid muscle and encompassed most areas of the pterygopalatine fossa. This distribution pattern within the infratemporal and pterygopalatine fossae is consistent with expectations [9], as the needle tip was positioned at the pterygomaxillary fissure, with bony structures preventing direct entry into the fossa in all except two specimens. Kampitak et al. [10] reported a similar distribution of methylene

blue using the anterior infrazygomatic approach. Conversely, Echaniz et al. [21] observed limited spread near the maxillary nerve and almost no spread into the infratemporal fossa using the suprazygomatic approach. In both the anterior infrazygomatic and suprazygomatic approaches, the needle tip was reportedly positioned within the pterygopalatine fossa, suggesting that the precise positioning of the needle tip may result in different distribution patterns.

We also determined that variations in the final needle tip positioning (either within the pterygopalatine fossa or at the pterygomaxillary fissure) might have influenced the distribution pattern of the injectate. When the needle was positioned directly within the pterygopalatine fossa, a broader range of structures within the fossa, including the maxillary nerve, sphenopalatine ganglion, and maxillary artery, were stained, indicating more extensive spread of the injectate. In contrast, when the needle was positioned at the pterygomaxillary fissure, the spread was more localized, primarily affecting the lateral pterygoid muscle and surrounding regions. While both needle positions are feasible in clinical settings, precise needle placement using ultrasound guidance may be challenging, and the exact position within the fossa or at the fissure may not be reliably confirmed. Importantly, these changes were evident on iodinated contrast-enhanced CT performed immediately after injectate application but were not observed during anatomical dissection.

The volume of solution that should be administered is also not well defined. While 1 ml was used in this study to selectively evaluate the distribution pattern, clinical volumes typically range from 1.5–5 ml, often exceeding the pterygopalatine fossa's capacity, resulting in a more nonselective distribution to adjacent areas such as the infratemporal fossa and, in some cases, through the foramen rotundum. Nader et al. [22] administered 1.5 ml of contrast

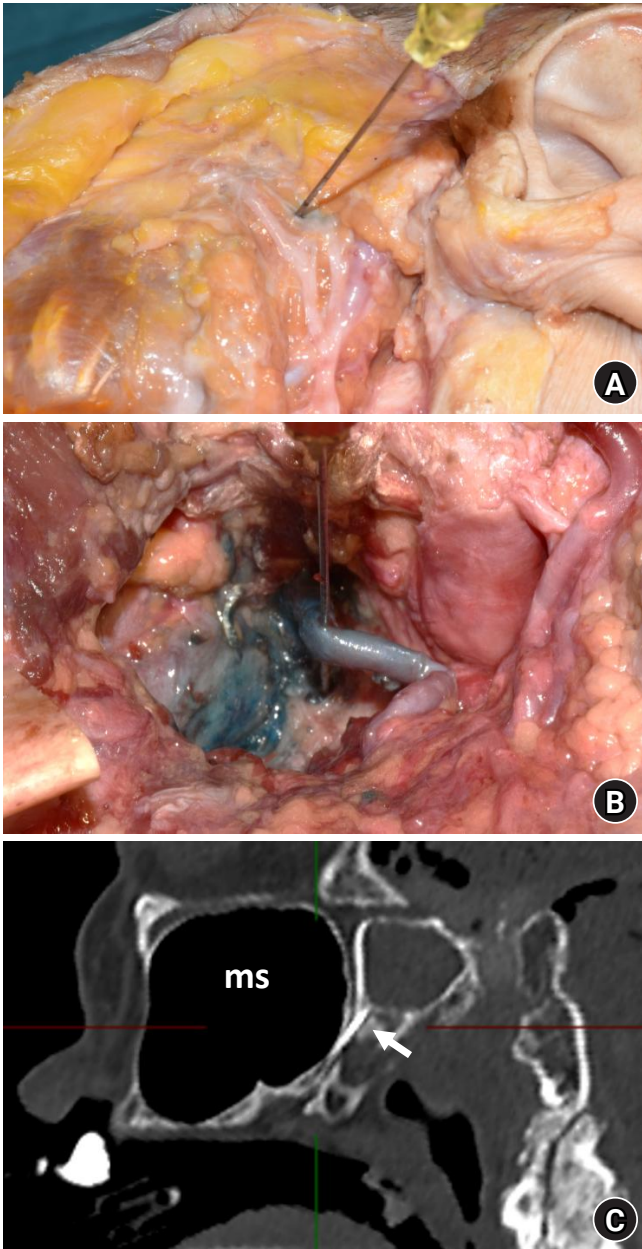


Fig. 2. Injuries associated with the posterior infrazygomatic and transoral approaches. (A) Injury to the temporal branch of the facial nerve (posterior infrazygomatic approach). (B) Perforation of the pterygoid portion of the maxillary artery within the infratemporal fossa (posterior infrazygomatic approach). (C) Needle penetrating the lateral pterygoid plate following the transoral approach, with contrast agent encompassing the medial pterygoid muscle (arrow). ms: maxillary sinus.

agent via the posterior infrazygomatic approach in a single patient, and detected its passage through the foramen rotundum using fluoroscopic guidance. Conversely, we noticed this spread via anatomical dissection in merely one specimen (8%). Interestingly, some authors have reported no evidence of spread through the foramen rotundum to the Gasserian ganglion after administering

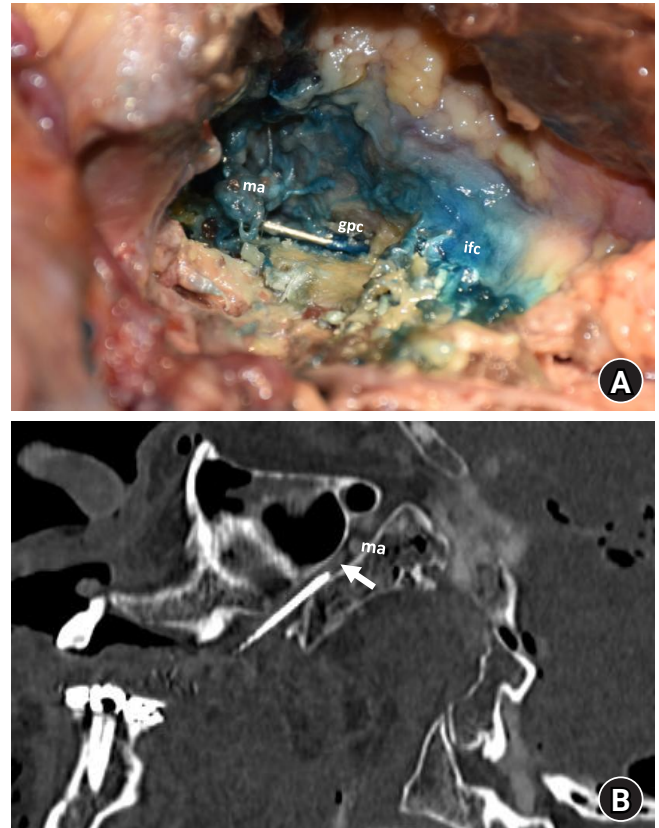


Fig. 3. Injectate distribution pattern following the transoral approach. (A) Maxillary artery, greater palatine canal, and infratemporal fossa stained with methylene blue. Note the needle position within the greater palatine canal after partial wall removal. (B) Computed tomography showing the needle within the greater palatine canal and contrast agent encompassing the inferior portion of the pterygopalatine fossa (arrow). ma: maxillary artery, gpc: greater palatine canal, ifc: infratemporal fossa content.

5 ml directly into the pterygopalatine fossa [21]. Similarly, we did not observe contrast spread to the Gasserian ganglion. This further suggests that discrepancies in spread may be influenced more by the needle tip position with different approaches through the pterygomaxillary fissure, rather than exclusively by the volume of the injectate.

In the transoral approach via the greater palatine canal, the injectate predominantly spreads within the inferior portion of the pterygopalatine and infratemporal fossae and along the needle trajectory. Angling the needle at 45° improved the safety of this approach by ensuring a consistent needle depth of 25 mm [19]. As the needle entered the pterygopalatine fossa at the inferior aspect, injectate distribution near the maxillary artery and within the greater palatine canal is consistent with expectations. Higher-volume injections could achieve a wider distribution, encompassing structures located in the superior regions of the pterygopalatine fossa, or, conversely, could spread via the pterygomaxillary fissure.

The differences in the distribution patterns of methylene blue and the iodinated contrast agent likely reflect their physicochemical properties and the different timing of evaluations. CTs were performed immediately after administration; therefore, a more localized distribution pattern was anticipated. Conversely, the methylene blue spread was evaluated during anatomical dissection, which was initiated after an interval, allowing for a broader distribution. The differences in the distribution patterns between the two agents may have also been influenced by the detection threshold. Although methylene blue can be easily visualized during anatomical dissection, larger quantities of the iodinated contrast agent are likely needed for its detection on CT. Furthermore, compared with amphipathic local anesthetics with distinct diffusion and distribution patterns [23,24], the hydrophilic nature of methylene blue and the high viscosity of iodinated contrast agents should be considered, as these properties could limit their spread. This is particularly important when comparing the results with clinical findings [25,26].

During the posterior infrazygomatic approach, the risk of puncturing the maxillary artery was assessed in accordance with a previous virtual reality study that evaluated 100 diagnostic CT angiographies. That study indicated that the artery enters the pterygopalatine fossa in the lower or anterior portion [13]; therefore, we aimed to introduce the needle into the posterosuperior portion of the accessible trajectory. Identifying the maxillary artery during ultrasonography was impeded by the fact that the Doppler mode cannot be used on cadaveric specimens. As this artery serves as an essential sonographic landmark for ultrasound-guided nerve blocks via the pterygomaxillary fissure [27], injury to the maxillary artery could plausibly have been avoided in a living subject.

No injuries to the maxillary artery were observed using the transoral approach, and the measured distance from the needle tip to the maxillary artery was relatively consistent. However, in one specimen, the lateral pterygoid plate was inadvertently injured during a transoral approach attempt, resulting in an altered distribution pattern of the iodinated contrast agent and methylene blue, encompassing the medial pterygoid muscle. Such complications might be expected in cases of fragile, cadaveric bone. In a clinical scenario, this could present as a lack of anesthetic effect or trismus due to injury to the medial pterygoid muscle. The relatively high rate of complications in this study is likely attributable, at least in part, to the limitations of the cadaveric model.

The primary limitation of this study was its *ex vivo* design, which does not fully replicate *in vivo* physiological conditions. Factors, such as active blood circulation, which is responsible for molecular clearance, and higher body temperatures, which can al-

ter injectate spread, are not present in an *ex vivo* setting. Another limitation was the presence of autolytic processes that affect smaller structures such as the palatine nerves, hindering thorough evaluations of potential injuries within the greater palatine canal. The greater palatine canal contains the palatine nerves and arteries, and the potential risks of puncturing these structures should be acknowledged. While using a fixed cadaveric material may be preferable for such assessments, it could also alter tissue properties and thus impact the distribution of the injectate. Future cadaveric studies should focus on evaluating the neurovascular structures within the greater palatine canal. Another limitation is the relatively small number of specimens, all of whom were elderly, which may influence generalizability due to age-related anatomical changes in the pterygopalatine fossa and thus limit the statistical power, all of which warrant interpreting the findings with caution.

In conclusion, the posterior infrazygomatic approach achieved a wider injectate distribution within the pterygopalatine fossa than the transoral approach, which primarily targets the inferior portion. The former is thus preferable when targeting the maxillary nerve, maxillary artery, or sphenopalatine ganglion, whereas the latter is better suited for the palatine nerves or the inferior portion of the fossa. Importantly, our findings indicate that the final needle position in the infrazygomatic approach, whether at the fissure or within the pterygopalatine fossa, can influence injectate distribution. These anatomical and technical nuances should be considered when choosing the best approach based on the clinical objectives.

Acknowledgements

We would like to thank Majda Črnak-Maasarani for technical support, Matej Cankar for assistance with anatomical dissection, and Chiedozie K. Ugwoke for proofreading the manuscript.

Funding

This research was supported by the Slovenian Research Agency grants J3-50106 and P3-0043.

Conflicts of Interest

No potential conflict of interest relevant to this article was reported.

Data Availability

The datasets generated during and/or analyzed during the current study are available from the corresponding author on reasonable request.

Author Contributions

Anže Jerman (Conceptualization; Data curation; Formal analysis; Investi-

gation; Methodology; Writing – original draft; Writing – review & editing)

Luka Pušnik (Conceptualization; Data curation; Formal analysis; Writing – original draft; Writing – review & editing)

Erika Cvetko (Conceptualization; Funding acquisition; Supervision; Writing – review & editing)

Nejc Umek (Conceptualization; Investigation; Methodology; Resources; Validation; Visualization; Writing – review & editing)

Žiga Snoj (Conceptualization; Funding acquisition; Methodology; Supervision; Writing – review & editing)

ORCID

Anže Jerman, <https://orcid.org/0000-0003-0816-3800>

Luka Pušnik, <https://orcid.org/0000-0003-3418-0348>

Erika Cvetko, <https://orcid.org/0000-0002-4414-5928>

Nejc Umek, <https://orcid.org/0000-0001-5831-2216>

Žiga Snoj, <https://orcid.org/0000-0001-6864-8880>

References

- Salgado-Parente A, González-Huete A, Antolinos-Macho E, Michael-Fernández A, Quintana-Pérez JV, Alba-Pérez B, et al. Radiologist's guide to the pterygopalatine fossa. *Radiographics* 2023; 43: e230078.
- Silveira-Bertazzo G, Martinez-Perez R, Carrau RL, Prevedello DM. Surgical anatomy and nuances of the expanded transpterygoid approach to the pterygopalatine fossa and upper parapharyngeal space: a stepwise cadaveric dissection. *Acta Neurochir (Wien)* 2021; 163: 415-21.
- Roberti F, Boari N, Mortini P, Caputy AJ. The pterygopalatine fossa: an anatomic report. *J Craniofac Surg* 2007; 18: 586-90.
- Nader A, Kendall MC, De Oliveria GS, Chen JQ, Vanderby B, Rosenow JM, et al. Ultrasound-guided trigeminal nerve block via the pterygopalatine fossa: an effective treatment for trigeminal neuralgia and atypical facial pain. *Pain Physician* 2013; 16: E537-45.
- Puthenveetil N, Rajan S, Mohan A, Paul J, Kumar L. Sphenopalatine ganglion block for treatment of post-dural puncture headache in obstetric patients: an observational study. *Indian J Anaesth* 2018; 62: 972-7.
- Lin C, Abboud S, Zoghbi V, Kasimova K, Thein J, Meister KD, et al. Suprazygomatic maxillary nerve blocks and opioid requirements in pediatric adenotonsillectomy: a randomized clinical trial. *JAMA Otolaryngol Head Neck Surg* 2024; 150: 564-71.
- Mesnil M, Dadure C, Captier G, Raux O, Rochette A, Canaud N, et al. A new approach for peri-operative analgesia of cleft palate repair in infants: the bilateral suprazygomatic maxillary nerve block. *Pediatr Anaesth* 2010; 20: 343-9.
- Wormald PJ, Athanasiadis T, Rees G, Robinson S. An evaluation of effect of pterygopalatine fossa injection with local anesthetic and adrenalin in the control of nasal bleeding during endoscopic sinus surgery. *Am J Rhinol* 2005; 19: 288-92.
- Anugerah A, Nguyen K, Nader A. Technical considerations for approaches to the ultrasound-guided maxillary nerve block via the pterygopalatine fossa: a literature review. *Reg Anesth Pain Med* 2020; 45: 301-5.
- Kampitak W, Tansatit T, Shibata Y. A cadaveric study of ultrasound-guided maxillary nerve block via the pterygopalatine fossa: a novel technique using the lateral pterygoid plate approach. *Reg Anesth Pain Med* 2018; 43: 625-30.
- Sola C, Raux O, Savath L, Macq C, Capdevila X, Dadure C. Ultrasound guidance characteristics and efficiency of suprazygomatic maxillary nerve blocks in infants: a descriptive prospective study. *Paediatr Anaesth* 2012; 22: 841-6.
- Jerman A, Janáček J, Snoj Ž, Umek N. Quantification of the interventional approaches into the pterygopalatine fossa by solid angles using virtual reality. *Image Anal Stereol* 2021; 40: 63-9.
- Jerman A, Umek N, Cvetko E, Snoj Ž. Comparison of the feasibility and safety of infrazygomatic and suprazygomatic approaches to pterygopalatine fossa using virtual reality. *Reg Anesth Pain Med* 2023; 48: 359-64.
- Hwang SH, Seo JH, Joo YH, Kim BG, Cho JH, Kang JM. An anatomic study using three-dimensional reconstruction for pterygopalatine fossa infiltration via the greater palatine canal. *Clin Anat* 2011; 24: 576-82.
- Robbins MS, Robertson CE, Kaplan E, Ailani J, Charleston L 4th, Kuruville D, et al. The sphenopalatine ganglion: anatomy, pathophysiology, and therapeutic targeting in headache. *Headache* 2016; 56: 240-58.
- Aoun G, Zaarour I, Sokhn S, Nasseh I. Maxillary nerve block via the greater palatine canal: an old technique revisited. *J Int Soc Prev Community Dent* 2015; 5: 359-64.
- Doomernik DE, Kruse RR, Reijnen MM, Kozicz TL, Kooloos JG. A comparative study of vascular injection fluids in fresh-frozen and embalmed human cadaver forearms. *J Anat* 2016; 229: 582-90.
- Renard Y, Hossu G, Chen B, Krebs M, Labrousse M, Perez M. A guide for effective anatomical vascularization studies: useful ex vivo methods for both CT and MRI imaging before dissection. *J Anat* 2018; 232: 15-25.
- Douglas R, Wormald PJ. Pterygopalatine fossa infiltration through the greater palatine foramen: where to bend the needle. *Laryngoscope* 2006; 116: 1255-7.
- Stojčev Stajčić L, Gačić B, Popović N, Stajčić Z. Anatomical study of the pterygopalatine fossa pertinent to the maxillary nerve block at the foramen rotundum. *Int J Oral Maxillofac Surg* 2010; 39: 493-6.
- Echaniz G, Chan V, Maynes JT, Jozaghi Y, Agur A. Ultrasound-guided maxillary nerve block: an anatomical study using the suprazygomatic approach. *Can J Anaesth* 2020; 67: 186-93.
- Nader A, Bendok BR, Prine JJ, Kendall MC. Ultrasound-guided pulsed radiofrequency application via the pterygopalatine fossa: a practical approach to treat refractory trigeminal neuralgia. *Pain Physician* 2015; 18: E411-5.

23. Abuzerr S, Darwish M, Mahvi AH. Simultaneous removal of cationic methylene blue and anionic reactive red 198 dyes using magnetic activated carbon nanoparticles: equilibrium, and kinetics analysis. *Water Sci Technol* 2018; 2017: 534-45.
24. Istenič S, Jerman A, Pušnik L, Stopar Pintarič T, Umek N. Transnasal spread of bupivacaine into the pterygopalatine fossa following endoscopically assisted cotton swab placement: a cadaveric study. *Reg Anesth Pain Med* 2025. Advance Access published on Mar 26, 2025. doi:10.1136/rapm-2025-106553.
25. Strichartz GR, Sanchez V, Arthur GR, Chafetz R, Martin D. Fundamental properties of local anesthetics. II. Measured octanol:buffer partition coefficients and pKa values of clinically used drugs. *Anesth Analg* 1990; 71: 158-70.
26. Smrkolj V, Pregeljc D, Kavčič H, Umek N, Mavri J. Micro-pharmacokinetics of lidocaine and bupivacaine transfer across a myelinated nerve fiber. *Comput Biol Med* 2023; 165: 107375.
27. Nader A, Schitteck H, Kendall MC. Lateral pterygoid muscle and maxillary artery are key anatomical landmarks for ultrasound-guided trigeminal nerve block. *Anesthesiology* 2013; 118: 957.